Splitting of an $s = 1$ Point Disclination into Half-Integer Disclinations upon Laser Heating of a Langmuir Monolayer

E. Hatta[†] and Th. M. Fischer*[,‡,§]

Graduate School of Engineering, Hokkaido University, Kita-ku, Sapporo, 060-8628 Japan, and Max Planck Institute of Colloids and Interfaces, Am Mühlenberg 1, D-14476 Golm, Germany

Received: November 27, 2002; In Final Form: March 13, 2003

Integer $s = 1$ point disclination textures of the molecular orientation of a pentacosadiynoic acid Langmuir monolayer split into two $s = {}^1/_2$ defects upon laser heating. We explain this behavior by a competition of the line tension of a π-wall of the c-director connecting both defects with the continuum orientation elastic energy. While the line tension causes an attraction, the orientation elastic energy mediates a repulsive interaction between the half-integer disclinations. Laser heating of the texture locally induces an anisotropic stress in the orientationally ordered solid phase, forcing the molecular orientation into the monolayer plane and thereby reducing the π-wall line tension.

Introduction

Many liquid condensed phases of two-dimensional (2D) Langmuir monolayers of simple amphiphiles[1] have a close resemblance to thermotropic liquid crystalline phases in three dimensions (3D). An ingredient of 2D or 3D layered (smectic) liquid crystals distinguishing them from nonlayered liquid crystals is the existence of hexatic phases with behavior intermediate between solids and liquids. Recently we have shown, using Langmuir monolayers of pentacosadiynoic acid, that orientational textures exist not only in hexatic but also in solid phases. In solid orientationally ordered phases it is possible to exert anisotropic mechanical stress (e.g., to stretch the film), which couples to the orientational degrees of freedom. Experiments of this kind have been carried out in liquid crystalline elastomers by Finkelmann et al.[2] and have been described theoretically by Golubovic and Lubensky.[3] Here we describe laser heating experiments on solid Langmuir monolayer textures and show that locally stretching the film by thermoelastic effects couples to the orientation of the amphiphiles and alters the texture of the monolayer.

The textures are usually characterized by the c-director, which is the averaged projection of the molecular axis of the rodlike molecules onto the film plane. The x and y components of the c-director are denoted by $\cos\varphi$ and $\sin\varphi$, respectively, where φ is the tilt azimuth angle. In our investigation we will focus on $s = 1$ point defects, where the director rotates by $\Delta\varphi = 2\pi$ along a closed path around the point defect. A rich variety of $s = 1$ point disclination textures have been predicted theoretically and observed experimentally. In hexatic thin films, Dierker et al.[4] observed the development of five $\pi/6$ walls extending from the defect center. Textures in hexatic domains coexisting with an isotropic surrounding exhibit a virtual $s = 1$ defect located at the domain boundary and coalescing with its virtual $s = 1$ image defect, effectively creating an $s = 2$ point disclination at the boundary. These textures, called boojums, have been observed in liquid helium[5] as well as in monolayers of fatty acids.[6,7] Due to a coupling between the hexatic bond orientational order and the c-director,[8] 6- and 7-fold segmented droplets of hexatic phase separated by $\pi/6$ walls were observed in monolayers of esters.[9] However, simple $s = 1$ splay disclinations observed in nematic liquid crystals[10] seem to be absent in hexatic liquid crystals. Also, isolated half-integer disclinations that are present in 3D nematics are forbidden in monolayers because an inversion of the c-director corresponds to physically distinct molecular orientations. Fractional disclinations may only occur in conjunction with string defects connecting different disclinations that add up to a global half (full) integer disclination of the liquid crystal (monolayer) texture.[11] Disclinations of the same sign repel, while the string is associated with a line tension and therefore leads to an attraction of the defects. How far fractional disclinations might separate, therefore, depends on the competition of the elastic repulsion and string attraction between the defects. In monolayers no string defects ending in a fractional disclination have been reported so far, presumably because the line tension is much stronger than the elastic repulsion. If one is looking for string defects in monolayers, one must find a means of softening the string tension. One way of doing so is using π-walls. π-Walls disappear when the molecules are tilted by 90° and the π-wall tension vanishes in this limit. In monolayers, due to steric reasons the tilt angle of the aliphatic tail in the condensed phases is less than 40°, and indeed $s = {}^1/_2$ disclinations do not play a role. However, by incorporating rod-shaped moieties into the center of the aliphatic chain, a planar order of such mesogenic units may overpower the order of the aliphatic chains and lead to an almost in-plane director of the amphiphilic molecules. Structural studies by Gourier et al.[12] could show that, in Langmuir monolayers of monomeric and polymerized 10,12-pentacosadiynoic acid (PCA), diacetylenic rods order in a planar geometry in a liquid condensed phase. Searching for $s = 1$ disclinations that unbind into two $s = {}^1/_2$ defects due to a softening of the connecting π-wall therefore seems promising in PCA. In this study we show that such kind of unbinding may be induced by exposing solid orientationally ordered PCA $s = 1$ disclination textures to thermoelastic stress.

[†] Hokkaido University.
[‡] Max Planck Institute of Colloids and Interfaces.
[§] Current address: Department of Chemistry and Biochemistry, The Florida State University, Tallahassee, Florida 32306-4390. E-mail: tfischer@chem.fsu.edu.

10.1021/jp0275701 CCC: $25.00
Published on Web 06/10/2003

Experimental Section

Thermomechanical experiments have been performed in monomeric and polymerized 10,12-pentacosadiynoic acid (PCA). Polydiacetylene single crystals, either in bulk or in Langmuir monolayers have received much attention[13−15] because they are model systems for investigating the physics of low-dimensional electrical[16,17] and optical[18,19] phenomena in organic polymers. The well-known fact of this monomer monolayer is that it is polymerized from the solid-state condition topochemically, i.e., polymerization may be inhibited if the tails of the molecules in the monomer monolayers are not oriented properly with respect to their neighbors. Here the focus is switched to the ability of PCA to form $s = 1$ point disclinations.

PCA was purchased from Wako Pure Chemical Industries, Ltd., and PCA monomers were spread onto pure water (Millipore Milli-Q at 18 MΩ) contained in a home-built Teflon trough. Benzene was chosen because larger domains can be obtained with this solvent. A 10 mM solution was spread onto the water surface (50 cm^2) until an average molecular area of 23 $Å^2$ was reached. The use of a concentrated solution confined to a small spreading area was crucial for the formation of stripe or point disclination textures.[20] Lower concentrations (say, ∼0.5−1 mM) resulted in mosaic textures. No specific precautions were taken to prevent oxygen-assisted polymerization of the monolayer. Polymerization of PCA was carried out at the water/air interface by 15 min exposure of the monolayer to a UV lamp (λ =254 nm, 12 W). The distance from the lamp to the monolayer surface was 15 cm.

The Langmuir monolayers were visualized by Brewster angle microscopy (BAM) by use of an Ar^+ laser. BAM converts variations of tilt azimuth into variations of gray value. The contrast of these images is maximal for a planar ordering and vanishes for zero tilt (homeotropic order). For the laser heating, the monolayer also was in addition exposed to a Nd:YAG IR laser focused on the water/air surface. A second 20× objective was added to the BAM with the focus ($\varnothing \approx 3\,\mu$m) arranged so that it coincided with the field of view of the Brewster angle microscope. The power P of the IR laser (after the objective) was adjustable between 50 mW and 2 W. The temperature increase ΔT at the center of the hot spot is $\Delta T = \gamma P$, with γ = 10 K/W. The BAM combined with the laser heating as well as the method for measuring the temperature rise has been described in detail elsewhere.[21]

Results

Brewster angle microscopy images of monomeric PCA (T = 18 °C, π = 25 mN/m) reveal that stripe textures[22] coexist with $s = 1$ point disclinations (Figure 1). Boojum-type textures (a virtual $s = {}^1/_2$ disclination located close to the boundary; see Figure 2) are observed on rare occasions (such textures are much more common for myristic and pentadecanoic acid). Upon polymerization, the contrast of the $s = 1$ disclination textures increases, presumably due to a change in tilt and/or an increase in the optical anisotropy.

Figure 1 shows the change in contrast upon rotation of the analyzer. In all experiments the contrast in the images can be inverted by rotating the analyzer of the BAM. Therefore the contrast is due to differences in the c-director, not due to differences in thickness. Depending on the analyzer position, two or four dark and bright brushes are seen in the BAM images as one circles around the defect. We analyzed the defect by assuming a variation of the tilt azimuth φ as

$$\varphi = \varphi_0 + \psi \tag{1}$$

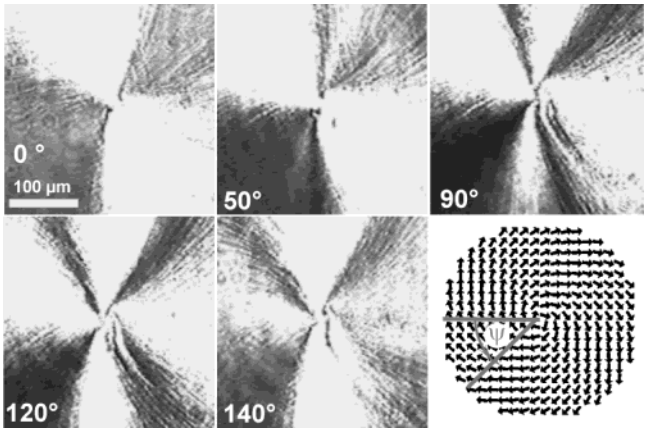

Figure 1. Brewster angle microscope images of the same $s = 1$ defect at different analyzer angle settings, $\alpha = 0°$, 50°, 90°, 120°, and 140°. For a broad range of analyzer settings, $50° < \alpha < 140°$, one observes four dark and four bright brushes in the image as one circulates around the defect center. This is a signature for a high tilt angle of the director. Analysis of the image reveals a spiral defect with an inclination angle of $\varphi_0 = -60°$, as sketched in the lower right panel.

where ψ denotes the polar angle in a polar coordinate system centered within the defect and measured with respect to the laser direction. In Figure 3 the polar angles ψ for which we observe bright and dark brushes are plotted as a function of the analyzer angle. The bright and dark brushes are expected for $\partial I/\partial\varphi = 0$, where I denotes the intensity of one pixel in the BAM image. By use of the Brewster angle reflection formulas,[23] this equation has two roots. For a fixed tilt azimuth φ, extinction brushes are predicted for analyzer angles α_{ext} that satisfy

$$\tan \alpha_{ext} = \frac{\cos^2 \varphi + b}{\sin \varphi (c + 2 \cos \theta_B \cos \varphi)} \tag{2a}$$

, and dark or bright brushes are predicted for analyzer angles α_{brush} that satisfy

$$\tan \alpha_{brush} = \frac{\sin 2\varphi}{(c \cos \varphi + 2 \cos \theta_B \cos 2\varphi)} \tag{2b}$$

where $\theta_B = 53.07°$ is Brewster's angle. The parameters b and c are fitting parameters related to the tilt angle ϑ, the dielectric constant perpendicular to the director is $\epsilon_\perp$, and the dielectric anisotropy $\delta\epsilon = \epsilon_{||} - \epsilon_\perp$ via

$$b = \frac{(\epsilon_\perp - 1)(\epsilon_\perp - \tan^2 \theta_B) + (\epsilon_\perp - 1 - \tan^2 \theta_B)\delta\epsilon \cos^2 \vartheta}{\epsilon_\perp \delta\epsilon \sin^2 \vartheta}$$

$$c = \frac{2 \tan \theta_B}{\epsilon_\perp \tan \vartheta} \tag{3}$$

Equation 2b is an implicit equation for a curve in the (α,φ) plane that starts as a bright brush in the origin and changes from a bright brush to a dark brush and vice versa each time it cuts the extinction brush (eq 2a) (Figure 3). We find agreement between experiment and the Brewster angle reflection formulas when choosing $\varphi_0 = -60°$, $\vartheta = 85° \pm 10°$, $\epsilon_\perp = 2$, and $\delta\epsilon$ = 0.6. The result of this fitting is shown in Figure 3.

In the fitting we have chosen a reasonable value for $\epsilon_\perp$. The fitting itself is not unique. There exists a one-parameter family of values ϑ, $\epsilon_\perp$, and $\delta\epsilon$, all resulting in the same value of b and c and resulting in the same brush positions. However, choosing a smaller tilt angle results in unreasonably high dielectric

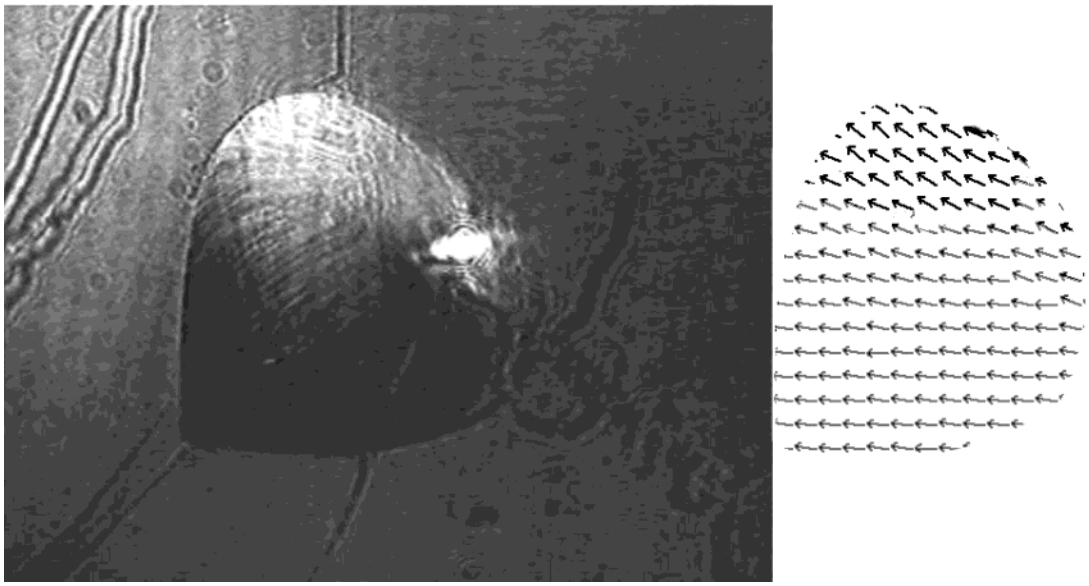

Figure 2. Brewster angle microscope image of a Boojum-type defect of pentacosadiynoic acid located at the boundary of the domain. The analyzer angle is $\alpha = 90°$. The texture giving rise to the variation in gray value of the image is sketched to the right. Turning the c-director of the sketched texture by multiples of $\pi/2$ leads to the same variation of the intensity, such that the texture is analyzed only modulo $\pi/2$.

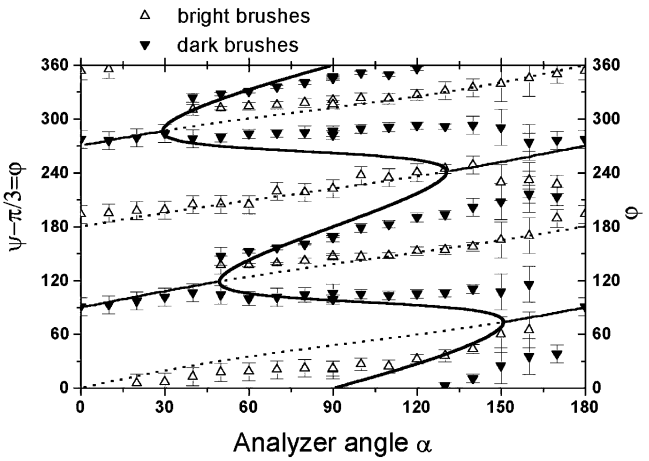

Figure 3. Analysis of the Brewster angle images of Figure 1. The polar angles $\psi - \pi/3$ at which one observes a dark (bright) brush in the image are measured as a function of the analyzer angle α. Theoretically extinction brushes (thick solid line) are predicted by eq 2a, and dark (solid line) and bright (dotted line) brushes are predicted by eq 2b, depending on how often the graph of eq 2b cuts the graph of eq 2a. The theoretical curves were obtained by the assumptions $\varphi = \psi - \pi/3$, $\vartheta = 85° \pm 10°$, $\epsilon_\perp = 2$, and $\delta\epsilon = 0.6$. The high tilt is in accordance with X-ray measurements[12] of the arrangement of the diacetylenic rods.

constants and dielectric anisotropies. Under this constraint, our best-fit analysis shows that the defect is an $s = 1$ spiral defect with an inclination angle of $-60°$. The tilt angle of the structure is close to 90°, such that the difference between the c-director and its mirror image is almost negligible. This result suggests that, in accordance with Gourier et al.,[12] most of the order arises from the planar arrangement of the diacetylenic rods in the molecules.

These results are strengthened by laser heating experiments, which locally exert anisotropic stress on the solid orientational defect. Figure 4 shows the central region of an $s = 1$ spiral defect before and after local heating ($\Delta T = 8$ K).

Prior to the heating, the intensity minima all meet at the central $s = 1$ singularity. After the heating, only two branches of the four minima meet at one point, indicating that the defect has split into two $s = {}^1/_2$ defects separated by approximately 5 μm. A π-wall between the defects cannot be resolved as the contrast between φ and $\varphi + \pi$ at tilt angles ϑ close to $\pi/2$ is too weak. The splitting is not reversible, and after the laser is switched off the two $s = {}^1/_2$ defects persist.

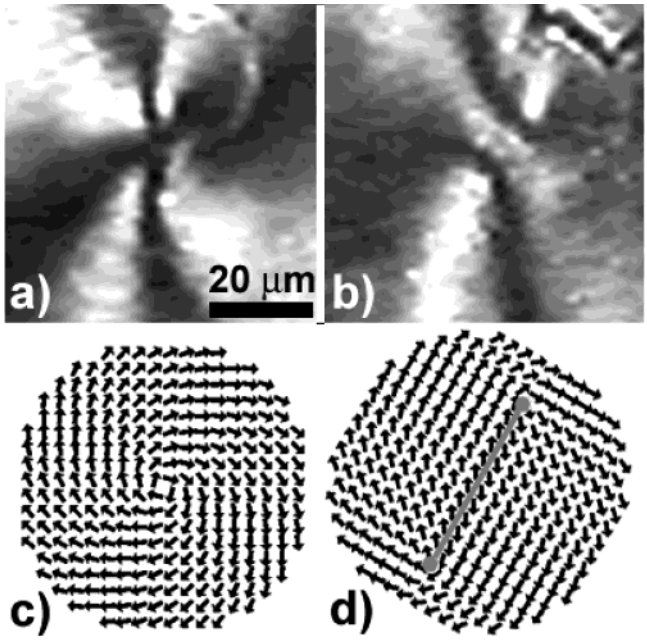

Figure 4. Brewster angle microscope images of the central region of a spiral defect in pentacosadiynoic acid (a) prior and (b) after local heating ($P = 0.77$ W corresponds to a local rise in temperature of $\Delta T = 8$ K). The $s = 1$ defect (a and c) splits in two $s = {}^1/_2$ defects (b and d). The π-wall between the defects cannot be resolved with the Brewster angle microscope as the tilt angle is close to 90°.

Theory

In this part we derive the orientation elastic energy and equilibrium separation of a two $s = {}^1/_2$ defect texture as sketched in Figure 4c,d. The arrows in Figure 4c,d are the c-director (projection of the director onto the monolayer plane). One anticipates that the energy of the π-wall is proportional to its length d:

$$F_\pi = \lambda d \tag{4}$$

where λ is the π-wall line tension. The energy of a texture with two $s = {}^1/_2$ defects can be calculated from the free energy:

$$F_{\text{elast}} = \frac{K}{2}\int d^2\mathbf{r}(\nabla\varphi)^2 \tag{5}$$

where K is the Franck elastic constant. The tilt azimuth field $\varphi(\mathbf{r})$ satisfies the Laplace equation:

$$\nabla^2\varphi = 0 \tag{6}$$

For two $s = {}^1/_2$ defects, neglecting effects from the domain boundaries, we may write

$$\varphi = \text{Im}\left(\ln\left[\left(z - \frac{d}{2}\right)\left(z + \frac{d}{2}\right)\right]\right) \tag{7}$$

where $z = x + iy$. The free energy of this structure is[24]

$$F_{\text{elast}} = 2E_{\text{core},1/2} + 2\pi K\left(\frac{1}{2}\right)^2\left[2\ln\frac{R}{a} - \ln\frac{d}{a}\right] \tag{8}$$

where a is a molecular cutoff, R is the radius of the domain, and $E_{\text{core},1/2}$ is the defect core energy. The energy has to be compared with the energy of a single $s = 1$ defect, which is

$$F_{\text{elast}} = E_{\text{core},1} + \pi K \ln\frac{R}{a} \tag{9}$$

Hence if $E_{\text{core},1} \approx 2E_{\text{core},1/2}$, splitting of an $s = 1$ defect into two $s = {}^1/_2$ defects lowers the energy. When the total free energy

$$F = F_\pi + F_{\text{elast}} \tag{10}$$

is minimized with respect to d, we find

$$d_{\min} = \frac{\pi}{2}\frac{K}{\lambda} \tag{11}$$

When the tilt ϑ approaches $\pi/2$, the difference between the c-director and its mirror image vanishes. This means that also the π-wall must disappear. In terms of a simple mean field approach, the line tension should vanish as

$$\lambda = \lambda_0\epsilon^{1/2} \tag{12}$$

for $\epsilon \rightarrow 0$, where we have introduced the control parameter:

$$\epsilon = 1 - 2\vartheta/\pi \tag{13}$$

measuring the deviation of the tilt angle from $\pi/2$. The parameter ϵ can be thought as well as $\epsilon = (\sigma - \sigma_c)/\sigma_c$, where σ is the stress created by the laser heating and σ_c is the critical stress required to force the molecules in plane. Inserting eq 12 into eq 11, one finds

$$d_{\min} = \frac{\pi}{2}\frac{K}{\lambda_0\sqrt{\epsilon}} \tag{14}$$

For $\epsilon \approx {}^1/_2$ (i.e., $\vartheta = \pi/4$), we expect microscopic separations between the defects, which is essentially an $s = 1$ defect (cf. Figure 4a), while when the molecules are forced in the monolayer plane $\epsilon \approx 0$ (i.e., $\vartheta = \pi/2$), the separation between the two $s = {}^1/_2$ defects grows macroscopically large. The local heating of the defect structure in Figure 4b presumably enforces such an in-plane orientation of the molecules via the stress created by the heating. Consequently a macroscopic separation into two $s = {}^1/_2$ defects is observed.

From studies of hexatic domains immersed into liquid phase, it is known that the line tension of interior domain walls ($\pi/3$ and π walls) must be smaller than the line tension between the hexatic liquid crystalline and the liquid phase.[8,9] This suggests[25] that the line tension λ_0 is smaller than 1 pN. For a liquid condensed phase we would expect a Franck elastic constant of the order $K \approx k_B T_c$, where $T_c \approx 300$ K is the hexatic to liquid transition temperature. Therefore, far away from the in-plane transition ($\epsilon \approx {}^1/_2$), the length d of the domain wall is expected to be of the order of some nanometers, while close to the transition ($\epsilon \approx 10^{-4}$) it grows to micrometers.

Conclusions

Brewster angle microscopy images of $s = 1$ point disclination textures of the molecular orientation of a pentacosadiynoic acid Langmuir monolayer suggest that the molecules are in a tilted orientationally ordered phase, with a tilt angle close to $\pi/2$. The order itself is predominantly due to planar arrangement of the diacetylenic rods in the molecule. These results are supported by experiments, where the solid phase is stretched irreversibly by local laser heating, which splits the defect into two $s = {}^1/_2$ defects. The experiments prove the existence of a new plastic solid orientationally ordered phase in two dimensions. If typical values for the Franck elasticity and the domain wall line tension are taken and continuum elastic theory is used, the growth of the π wall between the $s = {}^1/_2$ defects can be explained semiquantitatively.

Acknowledgment. We thank H. Möhwald for generous support and stimulating discussions. E.H. thanks the Max-Planck-Gesellschaft for providing a Max Planck fellowship. This work was supported by the Deutsche Forschungsgemeinschaft (DFG) with a Heisenberg Fellowship to Th.M.F. and by Grant Fi 548/3-1.

References and Notes

(1) Kaganer, V. M.; Möhwald, H.; Dutta, P. *Rev. Mod. Phys.* **1999**, *71*, 779.
(2) Finkelmann, H.; Kock, H. J.; Rehage, G. *Makromol. Chem. Rap.* **1981**, *2*, 317.
(3) Golubovic, L.; Lubensky, T. C. *Phys. Rev. Lett.* **1989**, *63*, 1082.
(4) Dierker, S. B.; Pindak, R.; Meyer, R. B. *Phys. Rev. Lett.* **1986**, *56*, 1819.
(5) Mermin, N. D. In *Quantum Fluids and Solids*; Trickey, S. B., Adams, E., Duffy, J., Eds.; Plenum: New York, 1977.
(6) Overbeck, G. A.; Möbius, D. *J. Phys. Chem* **1993**, *97*, 7999.
(7) Hénon, S.; Meunier, J. *J. Chem. Phys.* **1993**, *98*, 9148.
(8) Fischer, Th. M.; Bruinsma, R.; Knobler, C. M. *Phys. Rev. E* **1994**, *50*, 413.
(9) Knobler, C. M.; Desai, R. C. *Annu. Rev. Phys. Chem.* **1992**, *43*, 207.
(10) de Gennes, P. G.; Prost, J. *The Physics of Liquid Crystals*; Clarendon Press: Oxford, U.K., 1993.
(11) Pang, J.; Muzny, C. D.; Clark, N. A. *Phys. Rev. Lett.* **1992**, *69*, 2783.
(12) Gourier, C.; Alba, M.; Braslau, A.; Daillant, J.; Goldmann, M.; Knobler, C. M.; Rieutord, F.; Zalczer, G. *Langmuir* **2001**, *17*, 6496.
(13) Bloor, D.; Chance, R. R. *Polydiacetylenes: Synthesis, Structure, and Electronic Properties*; Martinus Nijhoff: Dordrecht, The Netherlands, 1985.
(14) Ulman, A. *Ultrathin Organic Films*; Academic Press: San Diego, CA, 1991.
(15) Prasad, P. N.; Williams, D. J. *Introduction to Nonlinear Optical Effects in Molecules and Polymers*; Wiley-Interscience: New York, 1991.
(16) Heeger, A. J.; *Rev. Mod. Phys.* **2001**, *73*, 681.
(17) Hoofman, R. J. O. M.; Siebbeles, L. D. A.; de Haas, M. P.; Hummel, A. *J. Chem. Phys.* **1998**, *109*, 1885.
(18) Osaheni, J. A.; Jenekhe, S. A.; Perlstein, J.; *J. Phys. Chem.* **1994**, *98*, 12727.

(19) Chemla, D. S., Zyss, J., Eds. *Nonlinear Optical Properties of Organic Molecules and Crystals*; Academic Press: San Diego, CA, 1987.
(20) Yamada, S.; Hatta, E.; Mukasa, K. *Jpn. J. Appl. Phys.* **1994**, *33*, 3528.
(21) Wurlitzer, S.; Lautz, C.; Liley, M.; Duschl, C.; Fischer, Th. M. *J. Phys. Chem.* **2001**, *B 105*, 182.
(22) Hatta, E.; Fischer, Th. M. *Langmuir* **2002**, *18*, 6201.
(23) Lautz, C.; Fischer, Th. M.; Weygand, M.; Lösche, M.; Kjaer, C.; Howes, P. *J. Chem. Phys.* **1998**, *108*, 4640−4646.
(24) de Gennes, P. G.; Prost, J. *The physics of liquid crystals*, 2nd ed.; Oxford Science Publications, Clarendon Press: Oxford, U.K., 1993; p 170ff.
(25) Wurlitzer, S.; Steffen, P.; Wurlitzer, M.; Khattari, Z.; Fischer, Th. M. *J. Chem. Phys.* **2000**, *113*, 3822−3828.